https://doi.org/10.5194/os-2020-112
Preprint. Discussion started: 16 December 2020

Ocean Science
Discussions
Open Access
EGU

Temporal and spatial variations in three-dimensional seismic oceanography

Zheguang Zou[1,2], Parsa Bakhtiari Rad[2], Leonardo Macelloni[3], and Likun Zhang[1,2]

[1]Department of Physics and Astronomy, University of Mississippi, University, MS 38677
[2]National Center for Physical Acoustics, University of Mississippi, 145 Hill Drive, University, MS 38677
[3]Hydrographic Science Research Center, School of Ocean Science and Engineering, The University of Southern Mississippi, 1020 Balch Blvd., Stennis Space Center, MS 39529

Correspondence: Likun Zhang (zhang@olemiss.edu)

Abstract. Seismic oceanography is a new cross-discipline between geophysics and oceanography that uses seismic reflection data to image and study the ocean water column. Previous works on seismic oceanography were largely limited to two-dimensional seismic data and methods. We present a complete three-dimensional (3D) oceanic seismic study and explore its imaging capability in seismic oceanography. From a 3D multichannel seismic survey acquired for oil and gas exploration in the Gulf of Mexico over six months period, a 3D water-column seismic volume was derived. The 3D seismic volume exhibits both temporal and spatial variations of the ocean, and theoretical and empirical analyses were performed to discriminate their contribution. Our analyses shows that temporal variation is largely embedded along crossline direction, showing discontinuities due to acquisition at varied times; however, inline sections, which can be seen as snapshot representation of the water column, allow to capture not only thermohaline structure but also the temporal evolution of the ocean dynamics. Our finding highlights that appropriately processed and analyzed 3D seismic data not only provide superior images of the ocean structure but also can be useful for investigation of temporal evolution of mesoscale ocean dynamics.

1 Introduction

Despite being the Earth's largest habitat by volume, the ocean water column remains one of the most poorly explored environments. Even where investigations are executed, physical, biological, and chemical parameters are generally derived over one-dimensional (1D) profiles (e.g. CTD casts, buoys and moorings) or two-dimensional (2D) transects (e.g. underwater gliders). Capturing the three-dimensional (3D) structure of the water column is extremely complicated: it can be reconstructed for a very large volume by combining 1D and 2D measurements, or, in a capacity limited to the surface water, it can be inferred from satellite observations. In addition, mesoscale and small-scale thermohaline fine structures are very difficult to observe with conventional methods whose lateral resolutions are low (usually $>$ 100 m). The ocean interior instead is 3D by nature and varies in both time and space on a wide range of scales. Features that affect thermohaline fine structures such as internal waves, solitons, tidal beams, eddies, and fronts are expected to vary both spatially and temporally.

Recent work has shown that marine seismic reflection profiling, a technique commonly used by geophysicists and geologists to image the Earth beneath the seafloor, can produce surprisingly detailed images of water-column structures. Holbrook et al.

https://doi.org/10.5194/os-2020-112
Preprint. Discussion started: 16 December 2020

(2003) and Holbrook and Fer (2005) demonstrated that 2D seismic reflection sections, if appropriately processed, provided very high-resolution images of the ocean structure, both vertical and, in particular, horizontal. Within the ocean water column, water density variations, fine scale (1-10 m thickness) temperature-salinity contrasts, and water turbidity fluctuations result in small changes in sound speed that produce weak, but distinct, sound reflections. These reflections, 100 to 1000 times weaker than those from the solid earth below, have generally been neglected by geophysicists, whose focus is the structure of the sub-seafloor. However, studies reveal that these reflections indeed correspond to ocean thermohaline structures (Nandi et al., 2004; Nakamura et al., 2006), primary (not completely) associated with temperature gradient (Ruddick et al., 2009). This new, cross-discipline between exploration seismology and physical oceanography, has come to be known as seismic oceanography (Holbrook et al., 2003) and has been successfully applied to imaging mesoscale and sub-mesoscale water-column structures such as ocean fronts (Gorman et al., 2018), eddies (Song et al., 2009; Tang et al., 2014a), internal waves (Holbrook et al., 2009; Tang et al., 2014b; Buffett et al., 2017), and other thermohaline fine structures (Holbrook et al., 2003). Additionally, several theoretical studies have been derived from the application of water-column seismic images including estimation of geostrophic currents (Sheen et al., 2011; Tang et al., 2014b), wave field spectra (Fortin et al., 2016), and internal wave mixing (Dickinson et al., 2017). Most of these studies used 2D seismic data and processing methods, but, in the modern exploration seismology of the oil and gas industry, 2D seismic methods are gradually upgraded to 3D seismic methods, which provide more adequate seismic images with the help of the additional dimension, leading to a more reliable interpretation (Yilmaz, 2001).

3D seismic is distinguished from 2D seismic by the contemporary acquisition of multiple closely spaced lines (e.g. 25 m) that provides regular data point spacing. This leads to a true data volume from which lines, planes, slices or probes can be extracted in any orientation, with nominally consistent data processing characteristics. While it is possible to acquire a dense, high-resolution grid of 2D lines, such grids are fundamentally different from a native 3D seismic survey (Lonergan and White, 1999; Yilmaz, 2001). The close line spacing of 3D seismic and the physical illumination of the subsurface from multiple offsets and multiple azimuths remove spatial aliasing problems inherent to 2D seismic data, therefore have the potential to yield better spatial resolution, useful for 3D seismic oceanography (Blacic and Holbrook, 2010). To date, 3D seismic oceanography is not well developed, which can be due to multiple facts: the 3D seismic data are very expensive to acquire, there is an interdisciplinary gap between oceanography and geophysics, and most importantly, a fundamental understanding of capability of 3D seismic oceanography is missing. The fundamental principle of exploration seismology assumes prevalently only spatial and not temporal variations in the subsurface (at least in the survey time frame). However, this issue challenges the development of 3D seismic oceanography, as 3D seismic surveys are generally acquired over a long period of time (e.g. from hours to months) and the water column may evolve during the collection of 3D seismic data. One fundamental question that must be answered for 3D seismic oceanography is: how are the temporal and spatial variations of the ocean dynamics imaged in a 3D seismic volume?

In this study, we present the results of a 3D seismic oceanography study carried out over a large deep-water area of the Northern Gulf of Mexico. We analyzed multi-directional seismic (inline, crossline and depth-slice) images and carried out both theoretical and empirical analyses with the aim of understanding the temporal and spatial variations in 3D seismic oceanography.

https://doi.org/10.5194/os-2020-112
Preprint. Discussion started: 16 December 2020

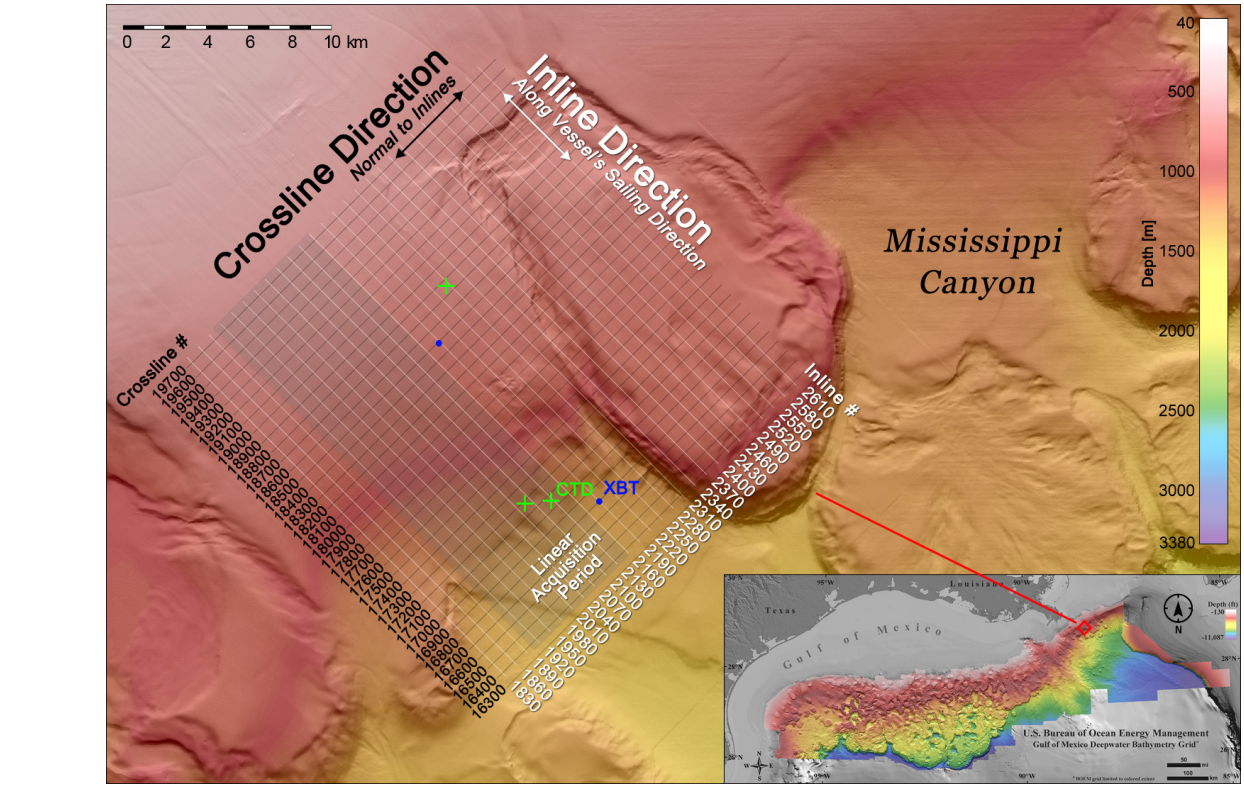

Figure 1. 3D seismic survey area with inline (white) and crossline (black) configuration, CTD (green cross) and XBT (blue dots) locations, and seafloor topography (background color). The 3D seismic survey area is marked by the grids. Inline is oriented to follow the continental slope. The inset shows the survey location in the Northern Gulf of Mexico. The seafloor topography data are provided by Bureau of Ocean Energy Management. The grey grids mark the linear acquisition period (explained in Sec. 2.4).

2 Data and Methods

2.1 3D Seismic Data

The seismic data used in this study are a portion of a large multichannel 3D seismic survey (Fig. 1) conducted by Schlumberger WesternGeco in the Northern Gulf of Mexico for oil and gas exploration between 2002 and 2003 . Survey lines run from northwest to southeast (inline azimuth, 330°) over a gentle slope (average inclination, 1.5°) where the seabed depth ranging from 800 m to 1300 m. Seismic data were collected using 2 airguns of 5085 cubic inch each in flip-flop configuration and 8 streamers, each accommodating 640 hydrophones. The streamer spacing is 100 m, and the hydrophone spacing is 12.5 m. We received the raw shot gathers sampled at 2 milliseconds (ms) and cut at the seafloor with no processing applied apart from analog to digital anti-aliasing (frequency range, 3-200 Hz) filter. We received multiple CTD and XBT casts, including three CTD and two XBT casts fall inside the seismic area (see Fig. 1).

https://doi.org/10.5194/os-2020-112
Preprint. Discussion started: 16 December 2020

2.2 3D Seismic Data Processing

Imaging the ocean water column using 3D seismic data from the oil industry is challenging. Acquisition geometry is not optimized for this target, and ocean internal reflections are inherently weak and masked by noises of different nature. However, oil industry contractors employ cutting edge technology and therefore the obtained seismic data are generally of very high quality. The seismic data processing was started with trace editing and amplitude balancing. We have removed offsets greater than 4 km (half of the total channel number) to keep computational cost low. The strong seafloor reflections were also muted to achieve a relative balance of amplitude levels. The data preprocessing used here employed standard techniques for subsurface seismic imaging, described in Yilmaz (2001), adapted to work with the water-column specific issues. Typical marine noises were present in the water-column data, e.g., acquisition-related noise, direct arrivals, reflection energy returns from previous shots, etc. Environmental noises include wind, shipping activity, and inherent ocean noise. We designed a filtering strategy specifically tailored to remove or minimize as much noise as possible while preserving the weak signals of interest. Consequently, we used low-cut 5 Hz and high-cut 150 Hz Butterworth filtering after each processing flow in various data domains to attenuate noise. The direct waves overlapped the subtle internal reflections of the water column and complicated the imaging. We applied frequency-wavenumber (FK) filtering and Radon filtering in different data domains to fruitfully attenuate unwanted linear noise, previous shot multiples, and seafloor refraction.

We processed the 3D data in a 3D fashion (which uses both inline and crossline data), rather than sequential 2D processing. The spherical divergence was compensated using the conventional exponential gain function (with power of 2) after some trials. For velocity analysis and normal move-out (NMO) correction, the data sort was changed to common-midpoint (CMP) and the semblance panels were produced in a window of 1410 to 1590 m/s. To build a reliable velocity model, sound velocity derived from CTD measurements were used to calibrate the seismic velocity model when there is a big mismatch. Afterwards, high coherence semblances were picked manually in a distance interval of every 250 m in both directions to model root-mean square (RMS) velocities for further processing. Accordingly stacking and time migration were performed using the RMS velocities in order to produce interpretable seismic images. We have also tested and performed a powerful multi-parameter imaging technique known as the common-reflection-surface (CRS) method for stacking and enhancing the data and also to avoid the NMO stretch effect (Yilmaz, 2001). The size of the CRS stacking surface was however chosen conservatively small in particular in the crossline direction (50 m) to avoid stacking traces from different swaths. The CRS showed improved results compared to the conventional CMP-based imaging especially along the inline direction (Bakhtiari Rad and Macelloni, 2020). Afterwards, post-stack time migration was performed using the estimated RMS velocities to correct the dipping events. Finally the data were time-to-depth converted using the estimated velocity function integrated with in situ sound velocity casts. More details of our seismic processing can be found in Bakhtiari Rad and Macelloni (2020).

2.3 3D Seismic Volume

The obtained 3D seismic volume of the ocean interior is illustrated in Fig. 2, showing the “slicing” configuration of 3D inline, crossline and depth-line seismic images. We use the chair-cut display to emphasize the multi-dimensional view. A 3D seismic

https://doi.org/10.5194/os-2020-112
Preprint. Discussion started: 16 December 2020

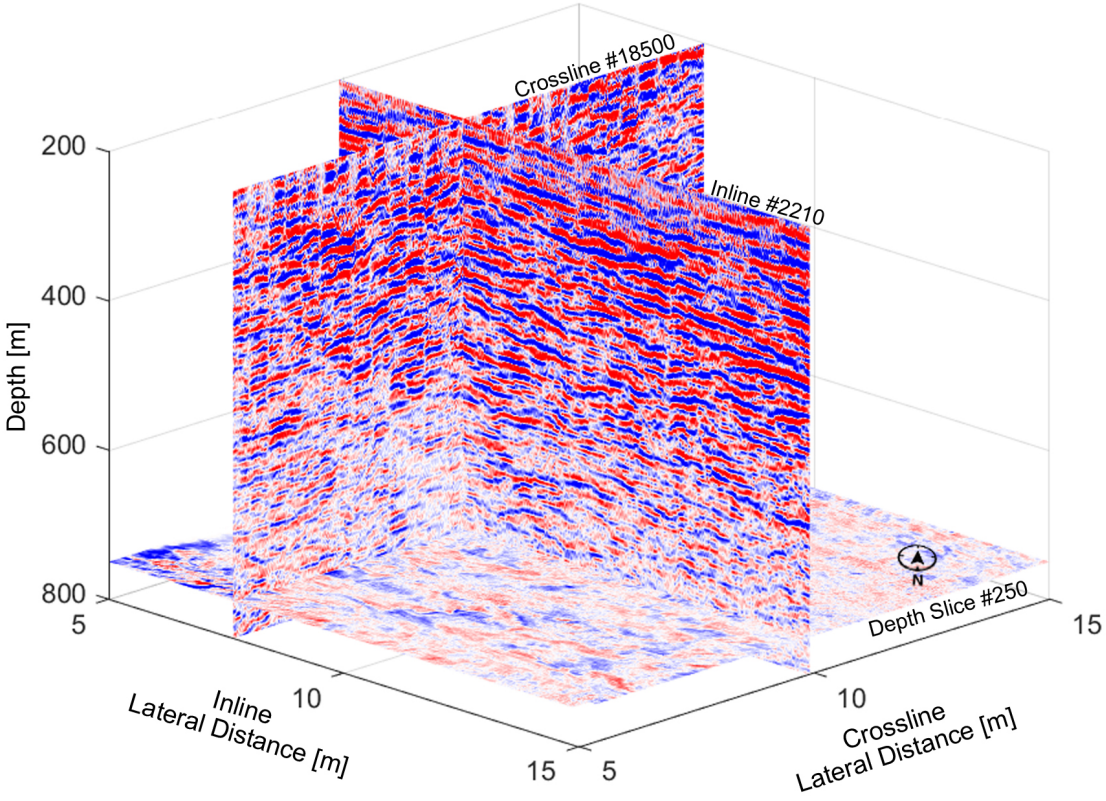

Figure 2. The inline, crossline and depth-slice configuration in our obtained water-column 3D seismic volume in the Gulf of Mexico. The lateral resolutions in inline and crossline directions are 6.25 m and 25 m, respectively, and the vertical resolution is 5 m. The color represents the amplitude of seismic reflection.

volume is generally a 3D matrix in which seismic reflections are color-coded according to the reflection amplitude and polarity. For seismic oceanography, changes in impedance contrast due to density and sound speed are due to changes in temperature and salinity in the water column (Ruddick et al., 2009). Because a seismic survey can be acquired in any planar directions, the notation in geographic coordinates (i.e., latitude and longitude) is not adopted, but instead the planar position is organized in *inline* (the direction along which the survey vessel tows the streamers) and *crossline* (perpendicular to inline); see Figs. 1 and 2. The volume has a spatial resolution of 6.25 m in inline, 25 m crossline, and 6-7 m in vertical direction (assuming sound speed of 1500 m/s and considering the dominant frequency of the airgun signal in the water column between 50 and 60 Hz). Our seismic volume shows only water columns below 200 m because the geometry of sources and receivers, optimized for subsurface deep targets (several kilometers below the seafloor), poorly image the shallowest portion of the water column (Piété et al., 2013). It is important to note that for a 3D seismic oceanography study, inline sections are generally acquired during a short temporal interval (typically a few hours considering the normal vessel velocity of 2.5 m/s), while crossline sections, which are obtained interpolating the inline sections perpendicularly, may embrace a wide temporal interval (up to several

https://doi.org/10.5194/os-2020-112
Preprint. Discussion started: 16 December 2020

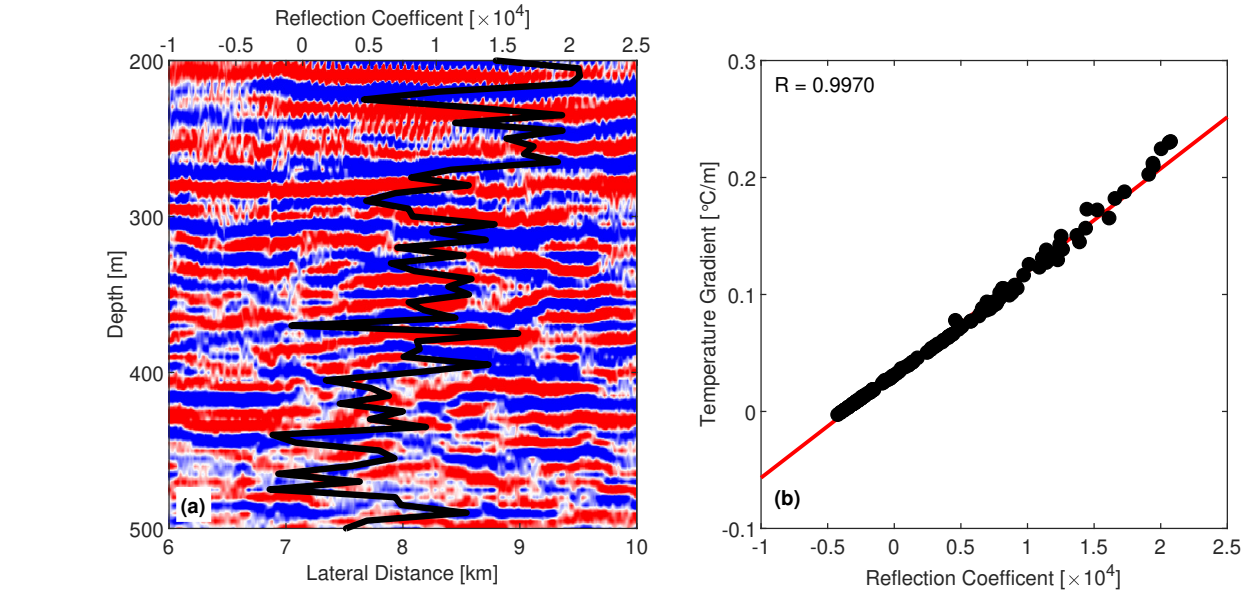

Figure 3. (a) Comparison of seismic imaging (Inline 2130) and the derived reflection coefficient (curve) from CTD data, both acquired on October 17, 2002. (b) Correlation between temperature gradient and the derived reflection coefficient between 200-1000 m.

months). We assume that water-column reflectors do not move during the shot and recording of the reflected signal (the stick slip model assumption (Klaeschen et al., 2009)). Considering our inline collection time (hours) is smaller than the timescale of the mesoscale ocean dynamics (days), we assume that each inline represents a seismic snapshot of the water column. The total volume consists of 821 inline images collected over about six months, from August 2002 to February 2003, with most collected between September and October.

2.4 Imaging Capability Analysis

To test if the 3D volume properly images the water column structures, we compared the seismic reflections with acoustic reflection coefficient derived by inverting the temperature salinity curves collected along the CTD profiles (Nakamura et al., 2006). The acoustic reflection coefficient for normal incident sound waves is given by (Kinsler et al., 1999):

$$R_s = \frac{\rho_1 c_1 - \rho_0 c_0}{\rho_1 c_1 + \rho_0 c_0} \tag{1}$$

where ρ_i and c_i are the density and sound speed of the medium with the subscript i specifies the medium. It has has been widely demonstrated that the amplitude of seismic reflections is largely related with the temperature gradients in the water column (Nandi et al., 2004; Nakamura et al., 2006; Ruddick et al., 2009), although sometimes salinity may play a role up to 40% in regions prone to diffusive convection (Sallarès et al., 2009). Figure 3 (a) compares the reflection coefficient derived from concurrent CTD measurements (collected on October 17, 2002, location shown in Fig. 1) with our seismic imaging (Inline #2130; seismic data collected on October 17, 2002). The overall agreement between the derived reflection coefficients with the

https://doi.org/10.5194/os-2020-112
Preprint. Discussion started: 16 December 2020

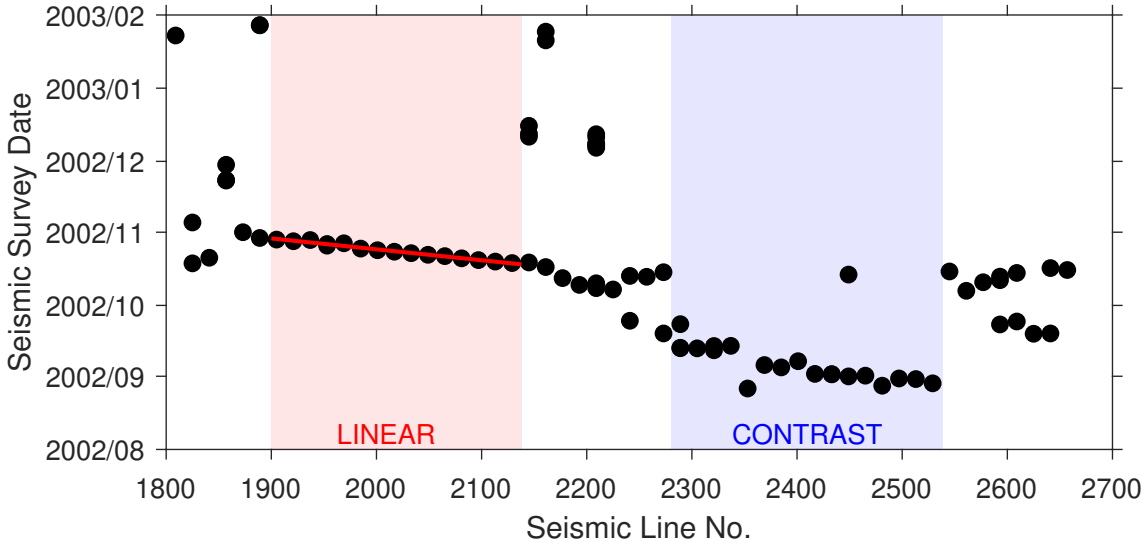

Figure 4. Dates of the seismic survey for the survey lines analyzed in our work. Two highlighted periods are a linear acquisition period (Lines # 1900-2130) during which data were collected linearly in time and space intervals, and a contrast acquisition period (Lines #2280-2540) which can display a huge time jump in seismic image. The line number here is equivalent to the inline number at the center of a seismic swath.

seismic reflections suggests that our 3D seismic data successfully represents water-column thermohaline structures. Also, the derived coefficient reflection highly correlate ($R = 0.9970$) with the temperature gradient [Fig. 3 (b)], suggesting that the color intensity in our seismic images can be interpreted as the vertical temperature gradient of the water column. In addition, the depth of the 3D volume seafloor reflection matches within 5-10 m error the seafloor depth from multibeam bathymetry which is derived using very high accurate sound speed measurements collected by NOAA's Ship Okeanos Explorer, suggesting that our migration is accurate and our seismic images accurately represent the water column structure.

2.5 Survey Line Analysis

Once we have established the oceanic natures of the seismic reflections, we attempt to address the correct relationship between time and space within our 3D seismic volume.

Again, we emphasize that inline sections are generally acquired during a short temporal interval (typically a few hours considering the normal vessel velocity of 2.5 m/s), while crossline sections, which are obtained by interpolating the inline sections perpendicularly, embrace a wide temporal interval, in our case up to several months. It has been demonstrated that water-column reflectors do not move during the very short time between the shot and the recording of the reflected signal (the stick slip model assumption (Klaeschen et al., 2009)). In 3D surveys each shot is recorded simultaneously along parallel streamers, swath, which for our data set count 8 streamers. To better understand the temporal distribution of the inline/swath, we carefully investigate the acquisition time for each survey line referring to the field acquisition records.

https://doi.org/10.5194/os-2020-112
Preprint. Discussion started: 16 December 2020

Figure 4 shows the seismic line number, which is equivalent to the center inline number of a seismic swath, as a function of the recording date and time. Considering that 3D surveys are ideally carried out by acquiring adjacent swaths consecutively, we should observe a linear relation between sailing line number and survey time. However, it is common that owing to operational problems (e.g., weather, maritime traffic, etc.) and/or bad data acquisition some portion of the area may be covered in a different time or some lines may be reacquired. Figure 4, indeed, shows a general linear trend, in particular for the portion including Lines 1900-2130. In this interval spatially contiguous seismic lines were collected consecutively in time. We refer this portion as *linear acquisition period* and we will use it in the correlation analysis discussed further.

3 Understanding 3D Seismic Water-Column Images

Before analyzing the temporal and spatial variation of an imaged oceanic 3D seismic volume, here we present our 3D seismic images to help readers to understand the fundamentals of 3D seismic oceanography. Our 3D seismic volume spatially extends for 480 km^3 of the water column in the Gulf of Mexico. It consists in 821 inline sections, 3,463 crossline sections and 256 depth slices. Temporally, it covers over six months following the pattern presented in Fig. 4.

Figure 5 shows three inline images, each representing a water-column snapshot at a location. For these inline sections, the temporal separation is 4 days while the spatial separation is 2.5 km. We observe layers of strong seismic amplitude in Fig. 5(a), moderate amplitude in Fig. 5(b), and weak amplitude in Fig. 5(c). The variation here is a result of changing temperature gradient (mostly, but not completely), not an artifact of differing processing parameters which were set the same for all inline sections. Considering the acquisition the time and location of these inline sections, we observe an variation of the ocean water column, not only spatially (over 5 km), but more importantly, temporally (over 8 days). Since the amplitude of seismic reflection is primarily associated with the vertical temperature gradient (in our region where salinity variation is small), this inline sequence illustrates a strong water-column mixing process: During the interval between October 20-28, 2002, over this portion (about 4 km) of the continental slope, strong and thick thermoclines gradually weakened and thinned, and eventually almost disappeared. Together, these 3D inline images suggest a *time-varying* mesoscale oceanographic process (length $>$ 10 km, depth $>$ 800 m, time $>$ 10 days) at the continental slope of the Northern Gulf of Mexico, transforming the water column from highly-stratified to well-mixed.

Figure 6 shows an example of our seismic crossline images. We observe significant discontinuities and a particular strong pattern of vertical stripes. The width of the stripes matches the swath width of the 3D seismic survey (0.4 km), suggesting that the discontinuity indicates temporal variation between the time of acquisition of these swaths. Swaths collected over the linear acquisition period (marked by the red line) display some continuity, but swaths collected with longer time difference can yield a significant discontinuity. For example, seismic imaging of the contrast acquisition period (marked by the blue line) looks drastically different from its neighboring parts due to a 20-day time shift (see Fig. 4). We also found that the discontinuity can vary with depth. The discontinuity is more significant at 200-350 m [Fig. 6(b)] than at 600-750 m [Fig. 6(c)], suggesting that temporal variation is more significant at shallow water column than the deep one. Notice that the seafloor is continuous, which is also proof of the discontinuity indicating the temporal variation, because the seafloor is associated with geological timescale

https://doi.org/10.5194/os-2020-112
Preprint. Discussion started: 16 December 2020

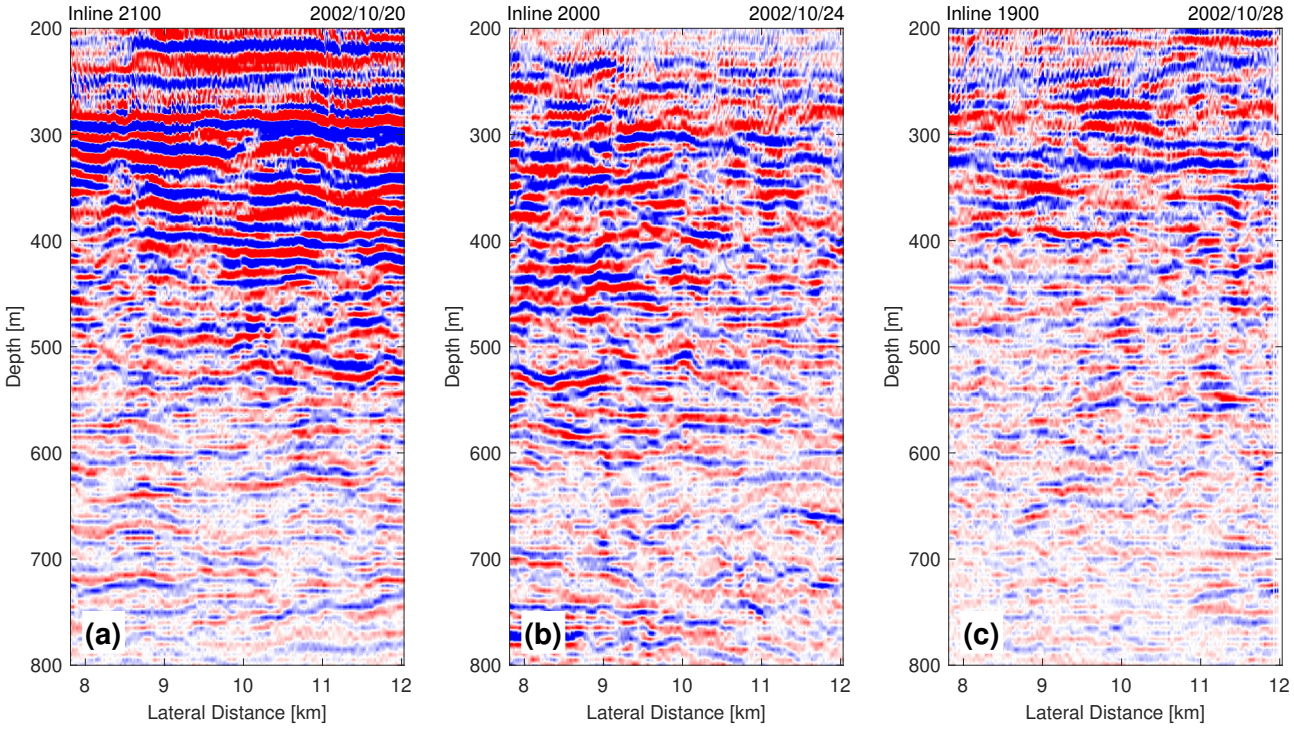

Figure 5. Three seismic inline images illustrating the temporal variation of the water column. (a) IL # 2100; (b) IL # 2000; (c) IL # 1900. Inline numbers and the date of collection are noted on the top. Temporal and spatial separation between images is 4 days and 2.5 km, respectively.

and there is no temporal variation in seafloor between seismic swaths. This analysis of crossline images suggest that temporal variation of the water column, appearing as image discontinuity, is significant in the crossline direction.

Figure 7 shows depth-slice images at three different depths: 250, 500 and 750 m. Water-column seismic depth slices are the most complex representation to conceptualize, since they offer a new representation of the ocean interior. We observe similar stripe pattern and the discontinuity appearing along the crossline direction. From shallow to deep layers, we see a decrease in discontinuity in the crossline direction. This decreased discontinuity agrees with the fact that the temporal variability of the top ocean is more significant than that of the deep ocean, as the ocean is mainly stirred from the top due to the wind-driven surface mixing (Talley et al., 2012). No significant discontinuity is seen along the inline direction. The analysis of depth-slice images suggests that the temporal variation of the ocean water column is non-negligible in the crossline direction, but negligible in the inline direction.

https://doi.org/10.5194/os-2020-112
Preprint. Discussion started: 16 December 2020

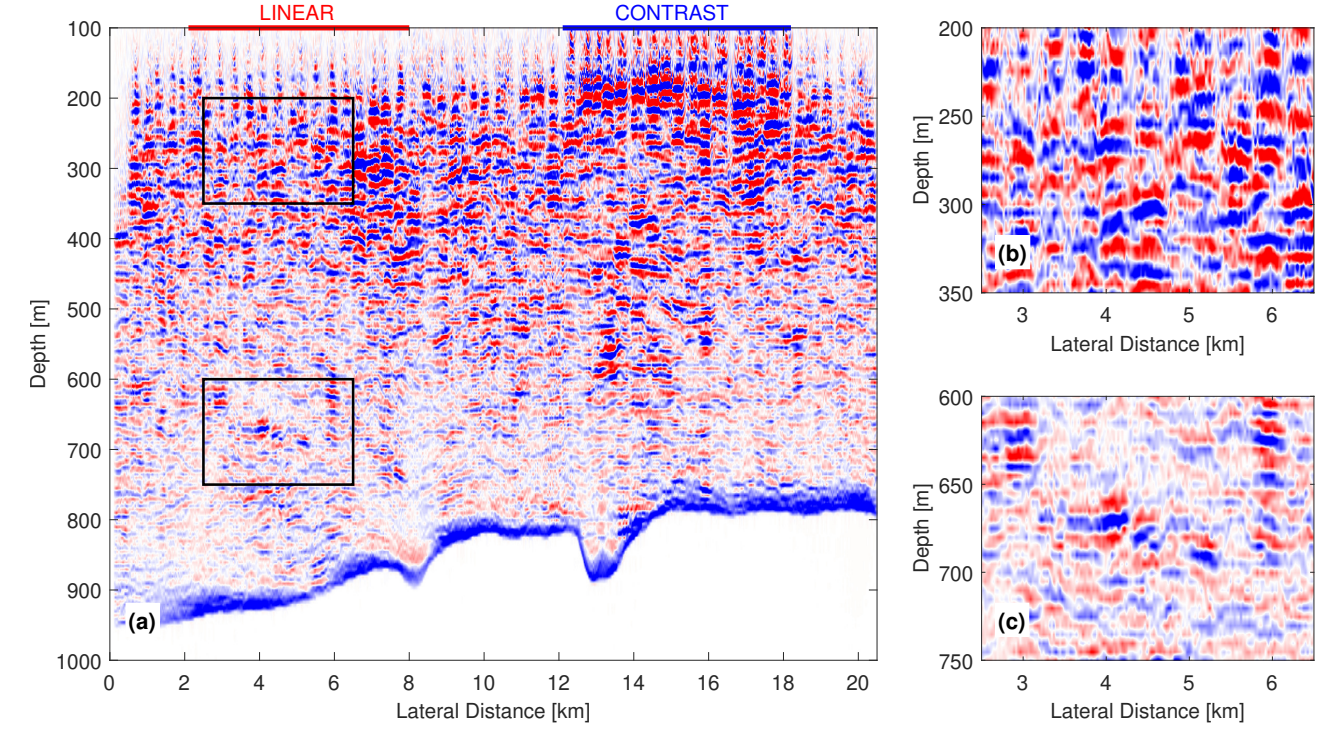

Figure 6. (a) An example of a crossline image (Crossline # 18200). (b) and (c) are close-up views of the regions shown in (a) for two different depths. The dates to collect the data span from August 2002 to February 2003. The red line at top marks the linear acquisition period, while the blue line marks the contrast period.

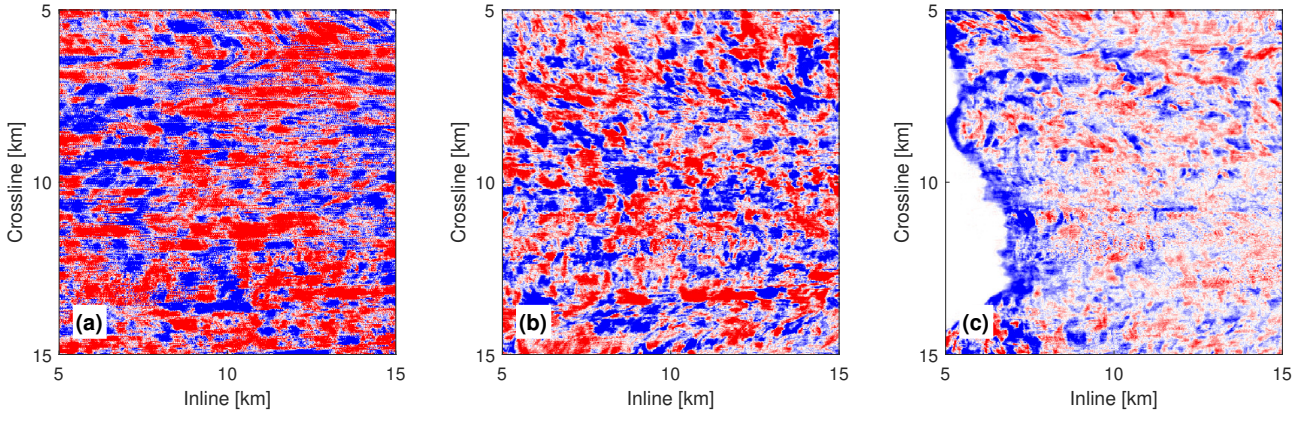

Figure 7. Seismic depth-slice images at three depths: (a) 250 m; (b) 500 m; (c) 750 m. The two axes shows the lateral distance in inline and crossline directions, respectively.

https://doi.org/10.5194/os-2020-112
Preprint. Discussion started: 16 December 2020

4 Temporal and Spatial Variations in 3D Seismic Oceanography

Our inline, crossline and depth-slice seismic images show that both spatial and temporal variation of the water column are embedded in a 3D seismic volume. Next, we conducted a theoretical and empirical analysis of the volume to understand the temporal and spatial variations in a 3D ocean seismic volume and to quantify their contributions.

4.1 Theoretical Analysis

Imagine a simple water column in which temporal variations are occurring at one cycle per day (1 cpd, about 10^{-5} Hz) and spatial variation at one cycle per kilometer (10^{-3} cpm). The values here are arbitrary but they can represent mesoscale oceanographic processes such as internal waves or internal tides (Talley et al., 2012), and seismic imaging is particularly useful for such processes.

We assume that this water column is imaged by an 3D seismic survey, having the same field geometry of our survey, and carried out swath-by-swath similar to the linear acquisition period. The vessel sails at a speed of 2 m/s, the seismic swath is 400 m wide, and the vessel is able to collect two swaths per day. Accounting for the two-way travel time, 1-km inline is collected in 10^3 s (about 0.012 day) and 1-km crossline spans 2.5 days (2.16×10^5 s). Based on these settings, the temporal, spatial and total (sum of both) variations in inline and crossline directions are illustrated in Fig. 8. We found that in inline direction [Fig. 8 (a)], the temporal component is subtle, and the total variation mostly follows the spatial component. In crossline direction [Fig. 8 (b)], however, the temporal variation is prominent, and the total variation is a fair combination of both temporal and spatial variations, with temporal variation being more noticeable. This theoretical analysis confirms that the 3D inline imaging mostly represents spatial variation, while the 3D crossline imaging represents a combination of both.

Further, we examine the wavenumber spectra of temporal and spatial variations for both directions [Figs. 8 (c) and (d)]. For spectral calculation we used the Fourier transform, and we used wavenumber domain instead of the frequency domain as the seismic images are intended to resolve spatial variations. We found that the spatial component appears at the correct location, at 10^{-3} cpm, in both directions, but the temporal component appears at two different locations – at about 10^{-5} cpm in the inline direction and at 2.5×10^{-3} cpm in the crossline direction. In other words, the temporal variation falsely shows up as a *low-frequency* component in the inline direction, being two orders (100 times) apart from the spatial component, but in the crossline direction, it appears as a *high-frequency* component, being only 2.5 times (in the same order) apart from the spatial component. Note that the dashed line in the inline spectrum only represents the theoretical prediction, which may not be successfully resolved if the seismic collection is too short (i.e., covering far less than a temporal cycle). This theoretical spectral analysis suggests that the temporal variation would be difficult to separate from spatial variation in the crossline direction because they are spectrally close to each other. In addition, the temporal variation would affect crossline imaging by posing a high-frequency aliasing.

https://doi.org/10.5194/os-2020-112
Preprint. Discussion started: 16 December 2020

Ocean Science
Discussions
Open Access
EGU

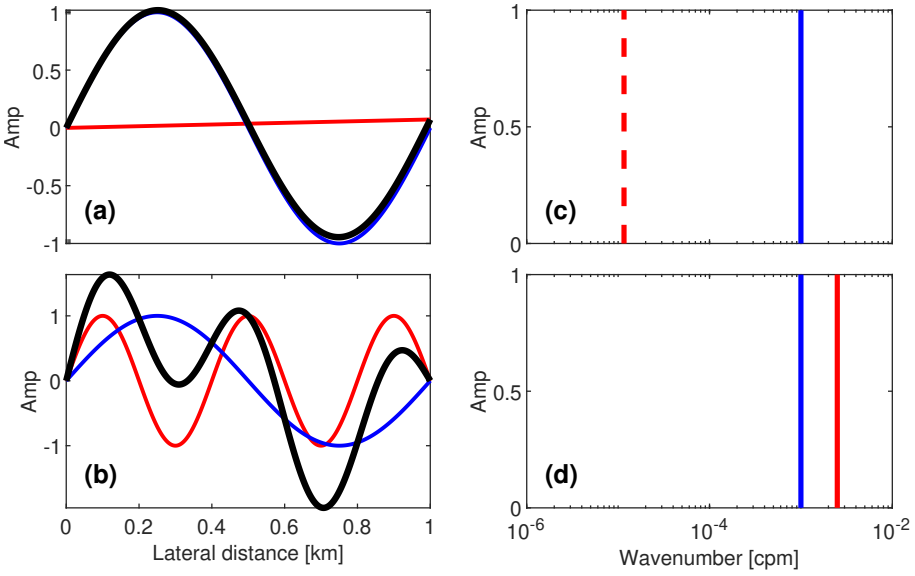

Figure 8. Illustration of temporal (red), spatial (blue) and total (black) variations in inline and crossline directions for a simple water column. (a) inline variation; (b) crossline variation; (c) spectrum of inline variation; (d) spectrum of crossline variation. Note that the dash line in (c) marked the theoretical position of temporal variations, which may not be resolved due to collection time.

4.2 Empirical Analysis

To analyze temporal and spatial variations in our 3D volume, we used the correlation function to quantify the variation in inline direction and crossline direction, namely *inline variation* and *crossline variation*, respectively. The cross-correlation is a measure of similarity between two variables. When the water-column structure varies, no matter temporally or spatially, the similarity between seismic images varies as well. Therefore, the change of the image similarity summarizes the variation of the water column. For 2D seismic images, x and y, the cross-correlation is defined as:

$$r = \sum_{i,j} \frac{(x_{ij} - \overline{x})(y_{ij} - \overline{y})}{\sigma_x \sigma_y} \tag{2}$$

where, i and j are the 2D index, $\overline{x}$ and $\overline{y}$ are the means, and σ_x and σ_y are standard deviations of x and y. The cross-correlation returns a scalar value between -1 and 1 to represent the imaging similarity, with +1 being exactly similar, -1 exactly reversed, and 0 being of no similarity. Noted that the cross-correlation is not affected by amplitude scale differences between different seismic images.

To obtain the cross-correlation of a seismic image series, we set the first image in the image series as reference or template and cross-correlate it with other images. In our analysis we set Inline 1900 and Crossline 18000 as the reference. Obtained cross-correlation is plotted as in terms of spatial distances or temporal shifts. The correlation length is defined as the length to the first zero crossing, suggesting the length that is required for two images to be completely different. The longer the

https://doi.org/10.5194/os-2020-112
Preprint. Discussion started: 16 December 2020

Ocean Science
Discussions
Open Access
EGU

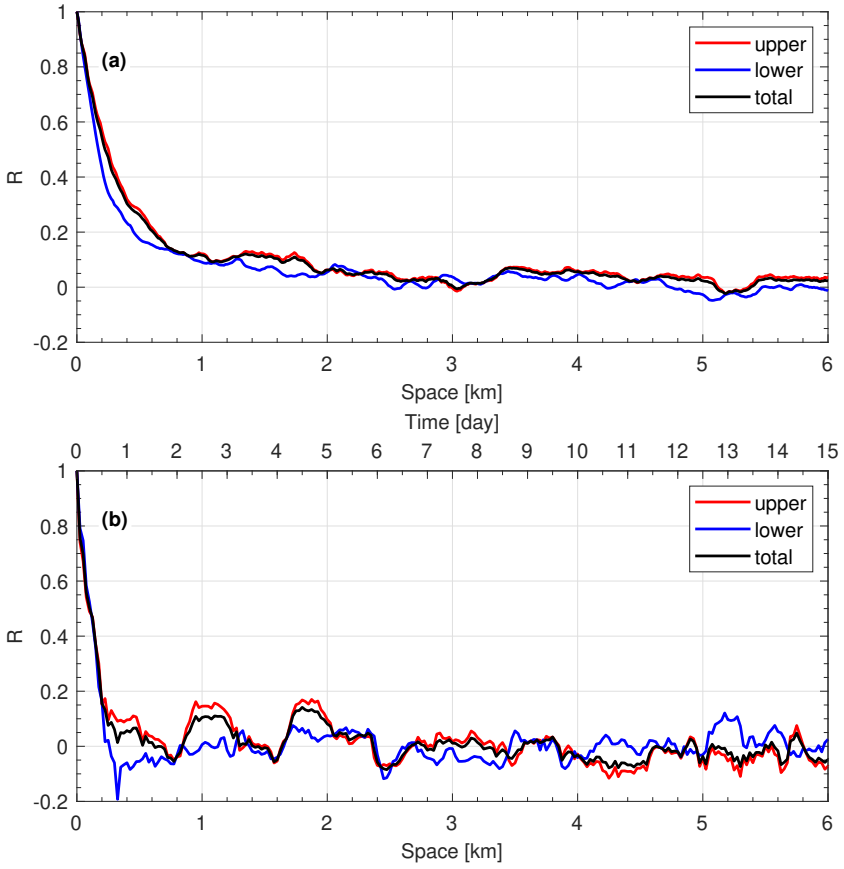

Figure 9. Correlation functions showing temporal and spatial variation in (a) inline and (b) crossline direction. Crossline variations are calculated within the linear acquisition period (Inline 1900-2140, see Fig. 4), and the inline variation is limited to 6 km for easy comparison with the crossline.

correlation length is, the slower the signal de-correlated. For periodical signal, the fluctuation of the correlation can be used to study the inherent cycles within the signal.

The inline (crossline) variation can be derived from 1D correlation between 1D traces within an inline (crossline) image. To achieve a higher dimensional accuracy, we use 2D correlation between multiple 2D images in the 3D seismic volume. In other words, an inline image is viewed as a trace (but extending in 2D space) in a crossline image. Therefore, crossline (inline) variation is the correlation between different inline (crossline) sections. Only the linear period (see Fig. 4) was used to perform the analysis. To best represent the variation of water column, we only use imaging of 250-750 m, excluding seafloors and low-quality shallow portion data. Furthermore, we divide the water column into two parts, the upper part (250-500 m) and the lower part (500-750 m), to explore the depth dependency.

Results for inline and crossline variations within our 3D seismic volume are shown in Fig. 9 (a) and (b), respectively. Here the variations are plotted as a function of space, and time (only for crossline). Overall, both inline and crossline variations

https://doi.org/10.5194/os-2020-112
Preprint. Discussion started: 16 December 2020

Ocean Science
Discussions
Open Access
EGU

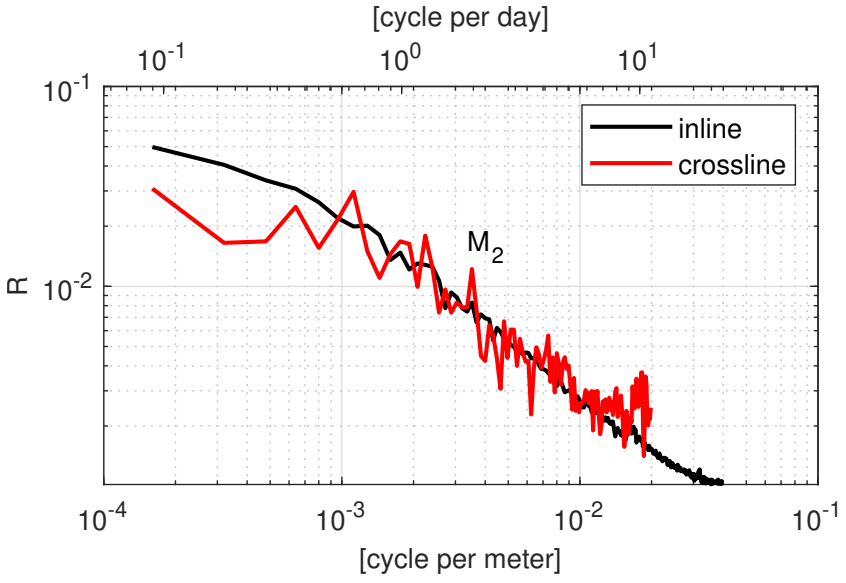

Figure 10. Spectra of the inline and crossline variations. The spectrum for the crossline variation is associated with both x-axes (time and space), while that for the inline variation is only associated with the lower x-axis only (space). The semi-diurnal (M2) tidal cycle is also denoted.

quickly decrease from unity and then gradually fluctuate up and down near zero as the space (i.e., lateral distance) increases. The upper and lower parts of the water column show different fluctuations, and the total variation for the whole water column is mostly dominant by the upper part. Comparing variations in these two directions, three observations can be made: (a) the crossline variation has larger fluctuations than the inline, (b) the crossline variation has a shorter correlation length (about 0.4 km) than the inline (about 2.5 km), and (c) the crossline variation has more high-frequency fluctuations than the inline. These observations confirm that the inline variation [Fig. 9(a)] is only associated with spatial variation, while the crossline variation [Fig. 9(b)] is associated with both temporal and spatial variations, since the increased fluctuation and decreased correlation length, due to the additional temporal variation, appear in the crossline direction.

Figure 10 further shows the inline and crossline spectra, calculated from the Fourier transform of the inline and crossline variations, respectively. Note that the inline is only associated with space, while the crossline is associated with both time and space. Overall, we observe a similar descending trend in both spectra. This decreasing trend suggests the spatial features in wavenumber domains. Comparing these two spectra, we observe many peaks in the crossline spectrum but not in the inline spectra. We suggest that these peaks represent the dominant frequencies of temporal variations. One particularly interesting observation is that the semi-diurnal tidal cycle (marked as M_2 in Fig. 10) appears in the crossline spectrum. This frequency is strong evidence that the crossline variation includes temporal variations, since coastal waters are often heavily influenced by tidal-forcing dynamics. Therefore, a significant amount of high-frequency components in crossline is definitely temporal variations, as suggested by our theory [Fig. 8 (d)] that the temporal variation will show up as a high-frequency aliasing in a

https://doi.org/10.5194/os-2020-112
Preprint. Discussion started: 16 December 2020

spatial spectrum. Our spectral analysis confirms that the crossline imaging captures temporal features of the ocean, while the inline imaging only captures the spatial features.

5 Discussion

The visual, theoretical and data driven analysis of the 3D seismic volume has provided a wealth of findings that we further discuss and summarize herein. Notice that this is a fairly new field, and we do not have a complete catalog of results and detailed concurrent oceanographic measurements that would allow unambiguously interpretation of the 3D seismic imaging in light of oceanographic processes.

Fundamentally, 3D seismic oceanography will be intrinsically affected by temporal variations, because ocean dynamics varies within a 3D seismic survey. Ideally one can design a 3D seismic survey that could optimally image an oceanographic process; knowing the periodicity, the spatial dimensions and the predominant season of the process, the acquisition geometry could be optimized. 3D seismic surveys are very expensive to collect and, in most of the case, we have to rely on data acquired for other purposes. 3D seismic surveys conducted for oil and gas exploration, cover a very large volume of ocean water and have the right bandwidth to depict water column reflections, but those surveys often are acquired over time which spans from days to months, we have to look for the oceanographic signals embedded in the seismic data and build the best processing and analysis workflow to extract it. Mesoscale and sub-mesoscale ocean dynamics (e.g., fronts, eddies, internal waves, turbulence, etc) hold a temporal variation of 10^{-6}–10^{2} Hz and a spatial variation of 10^{-4}–10^{2} cpm (Talley et al., 2012; Ruddick, 2018). As a result, wave spectra resulting from mismatched imaging inevitably produces a significant overlap of temporal variations on top of the spatial variation, therefore the temporal variation on 3D imaging may vary case by case, dataset by dataset, volume by volume.

In standard 3D seismic data processing for earth interior imaging, reflections within a large volume of subsurface are utilized and accounted for the out-of-plane acoustic scattering, to provide higher quality images than those resulting from 2D data. The general rule is to avoid summing inconsistent reflections from different seismic swaths. This is not always possible for the water column because of the temporal variation. Narrow aperture 3D multiparametric stack (Bakhtiari Rad and Macelloni, 2020) or swath-by-swath common mid-point 3D stacking (Blacic and Holbrook, 2010) can both be used to create 3D seismic oceanographic images because both implement a time-dependent selection for the seismic data. However, the processing workflow for 3D seismic oceanography can be case-dependent, and we suggest to perform always an in-depth temporal analysis to avoid to sum time-inconsistent seismic data.

Generally we found that:

Inline images are not affected by temporal variation (unless the inline is very long or is imaging fast-moving water-column structures (Klaeschen et al., 2009). Each inline can be seen as a snap shot of the water column vertical thermocline structure at a given time over a given location. This temporal and spatial heterogeneity cannot be fully separated, because this temporal evolution occurs at different locations. However, available data analysis methods (e.g. wave spectral analysis (Holbrook et al., 2013) and diffusivity estimations (Fortin et al., 2017; Dickinson et al., 2017)) developed for 2D seismic oceanography can be

https://doi.org/10.5194/os-2020-112
Preprint. Discussion started: 16 December 2020

safely extended to 3D inline images. Most importantly, because an inline section "samples" the ocean at one given time and one given place, we could have a particular sequence of inline images that adequately image both the spatial and temporal variations of oceanographic process. This knowledge can be applied to understand the temporal dynamics of mesoscale eddies and internal waves, as the evolution of their vertical structures are very difficult to capture using traditional in-situ oceanographic measurements. Recent 3D seismic oceanography studies with the *time-lapsing* concept (Dickinson et al., 2020; Gunn et al., 2020) are examples of application of this temporal variability in oceanographic studies. This temporal feature makes 3D seismic oceanography an extremely powerful tool for studying temporal evolution of mesoscale ocean dynamics.

Crossline sections carry both temporal and spatial information. Temporal variation being more prominent than spatial variation in the crossline direction is validated by the discontinuity in crossline images (Fig. 6), faster fluctuation in correlation function analysis in crossline direction (Fig. 9), and verified by theoretical analysis [Figs. 8 (b), (d)]. In contrast, if temporal variation of an imaged structure is less prominent, it would be buried under spatial variation without showing any discontinuity in crossline imaging. For example, the seafloor appears highly continuous (does not exhibit temporal variations) in our crossline imaging (Fig. 6) because it is associated with a long geological timescale longer than years. In general, ocean crossline images appear as low quality seismic images. This is mostly due to the temporal variation induced discontinuity, rather than fewer receivers in the crossline direction than in the inline direction (8 vs 640). Therefore, the low quality cannot be improved through common processing techniques such as trace interpolation (Yilmaz, 2001). Instead, the crossline imaging can only be improved by optimized 3D seismic survey configurations specifically designed for seismic oceanography, e.g., faster data collection across swaths. Nevertheless, crossline imaging still provide valuable information, offering an immediate overview of the temporal distribution of the seismic survey. Cross-correlation analysis helps to identify the sub portion in inline images that can be used in sequence.

In depth-slice images, temporal variation is present in the crossline direction, and is highly depth-dependent. This depth dependency comes from the timescale of ocean dynamics occurred at different depths. Due to water mixing of surface wind-waves, the top water column is usually highly dynamic, while the deep water is associated with a very long timescale (Talley et al., 2012). Such a depth dependence, in terms of imaging discontinuity, can be seen in the crossline images (Fig. 6) and depth-slice images (Fig. 7), which is also an evidence of the presence of temporal variation in the crossline direction. This depth dependency in 3D seismic oceanography can be a potential indicator to study the timescale of ocean dynamics at different depths.

6 Conclusions

This study focuses on 3D seismic oceanography and attempts to understand the spatial and temporal oceanographic signal embedded in 3D seismic data collected for oil and gas exploration. A complete 3D seismic volume of the Northern Gulf of Mexico water column has been presented, and 3D seismic images have been investigated for the first time using theoretical analysis and a correlation-based data analysis. Our results show that 3D oil industry seismic data carry a wealth of oceanographic information if appropriately processed and analyzed. However, it is important to analyze the temporal variation within

https://doi.org/10.5194/os-2020-112
Preprint. Discussion started: 16 December 2020

a 3D seismic volume before the interpretation of 3D seismic images and the analysis of wave fields in the seismic images. In this study, cross-correlation analysis is used as an effective tool to access the temporal and spatial information within the seismic volume.

This study illustrates how one can interpret 3D seismic data as spatio-temporal evolution of ocean interior structure, which is important to promote the use of 3D seismic oceanography. The fundamental understanding of temporal and spatial variation in 3D seismic oceanography is useful for 3D seismic oceanography studies in general and essential for the interpretation and analysis of 3D oceanic seismic images. It allows the extension of previous 2D seismic oceanography analysis, such as wave spectral analysis and diffusivity estimations, to 3D inline images, and to study the evolution of time-varying mesoscale ocean dynamics. Our future 3D seismic oceanography research will focus on investigation of the evolution of mesoscale ocean dynamics (eddies and internal waves) in the Northern Gulf of Mexico.

Data availability. The seismic data for this project were provided by Schlumberger Western Geco. The data are available from Schlumberger Multiclient Seismic Data Library (http://www.multiclient.slb.com; area MC-14Q).

Author contributions. ZZ and LZ conducted seismic imaging analysis. PBR and LM performed 3D seismic data processing and imaging.

Competing interests. The authors declare that they have no conflict of interest.

Acknowledgements. We would like to thank Schlumberger for providing the 3D seismic data. The seismic data were processed with software Vista from Schlumberger, Kingdom by IHS Markit, Seismic Unix from Colorado School of Mines. The 3D CRS program used in this study was developed by the Wave Inversion Technology (WIT) Consortium, Hamburg, Germany. This work was supported by the National Oceanic and Atmospheric Administration (NOAA) grant (NA17OAR011021).

https://doi.org/10.5194/os-2020-112
Preprint. Discussion started: 16 December 2020

References

Bakhtiari Rad, P. and Macelloni, L.: Improving 3D water column seismic imaging using the Common Reflection Surface method, Journal of Applied Geophysics, 179, 104 072, https://doi.org/10.1016/j.jappgeo.2020.104072, 2020.

Blacic, T. M. and Holbrook, W. S.: First images and orientation of fine structure from a 3-D seismic oceanography data set, Ocean Science, 6, 431–439, https://doi.org/10.5194/os-6-431-2010, 2010.

Buffett, G. G., Krahmann, G., Klaeschen, D., Schroeder, K., Sallarès, V., Papenberg, C., Ranero, C. R., and Zitellini, N.: Seismic oceanography in the Tyrrhenian Sea: thermohaline staircases, eddies, and internal waves, Journal of Geophysical Research: Oceans, 122, 8503–8523, https://doi.org/10.1002/2017JC012726, 2017.

Dickinson, A., White, N. J., and Caulfield, C. P.: Spatial variation of diapycnal diffusivity estimated from seismic imaging of internal wave field, Gulf of Mexico, Journal of Geophysical Research: Oceans, 122, 9827–9854, https://doi.org/10.1002/2017JC013352, 2017.

Dickinson, A., White, N. J., and Caulfield, C. P.: Time-Lapse Acoustic Imaging of Mesoscale and Fine-Scale Variability within the Faroe-Shetland Channel, Journal of Geophysical Research: Oceans, https://doi.org/10.1029/2019jc015861, 2020.

Fortin, W. F., Holbrook, W. S., and Schmitt, R. W.: Mapping turbulent diffusivity associated with oceanic internal lee waves offshore Costa Rica, Ocean Science, 12, 601–612, https://doi.org/10.5194/os-12-601-2016, 2016.

Fortin, W. F., Holbrook, W. S., and Schmitt, R. W.: Seismic estimates of turbulent diffusivity and evidence of nonlinear internal wave forcing by geometric resonance in the South China Sea, Journal of Geophysical Research: Oceans, 122, 8063–8078, https://doi.org/10.1002/2017JC012690, 2017.

Gorman, A. R., Smillie, M. W., Cooper, J. K., Bowman, M. H., Vennell, R., Holbrook, W. S., and Frew, R.: Seismic characterization of oceanic water masses, water mass boundaries, and mesoscale eddies SE of New Zealand, Journal of Geophysical Research: Oceans, 123, 1519–1532, https://doi.org/10.1002/2017JC013459, 2018.

Gunn, K. L., White, N., and Caulfield, C. c. P.: Time-Lapse Seismic Imaging of Oceanic Fronts and Transient Lenses Within South Atlantic Ocean, Journal of Geophysical Research: Oceans, 125, 1–26, https://doi.org/10.1029/2020JC016293, 2020.

Holbrook, W. S. and Fer, I.: Ocean internal wave spectra inferred from seismic reflection transects, Geophysical Research Letters, 32, 2–5, https://doi.org/10.1029/2005GL023733, 2005.

Holbrook, W. S., Páramo, P., Pearse, S., and Schmitt, R. W.: Thermohaline fine structure in an oceanographic front from seismic reflection profiling, Science, 301, 821–824, https://doi.org/10.1126/science.1085116, 2003.

Holbrook, W. S., Fer, I., and Schmitt, R. W.: Images of internal tides near the Norwegian continental slope, Geophysical Research Letters, 36, 1–5, https://doi.org/10.1029/2009GL038909, 2009.

Holbrook, W. S., Fer, I., Schmitt, R. W., Lizarralde, D., Klymak, J. M., Helfrich, L. C., and Kubichek, R.: Estimating oceanic turbulence dissipation from seismic images, Journal of Atmospheric and Oceanic Technology, 30, 1767–1788, https://doi.org/10.1175/JTECH-D-12-00140.1, 2013.

Kinsler, L. E., Frey, A. R., Coppens, A. B., and Sanders, J. V.: Fundamentals of acoustics, Fundamentals of Acoustics, 4th Edition, by Lawrence E. Kinsler, Austin R. Frey, Alan B. Coppens, James V. Sanders, pp. 560. ISBN 0-471-84789-5. Wiley-VCH, December 1999., p. 560, 1999.

Klaeschen, D., Hobbs, R. W., Krahmann, G., Papenberg, C., and Vsemirnova, E.: Estimating movement of reflectors in the water column using seismic oceanography, Geophysical Research Letters, 36, https://doi.org/10.1029/2009GL038973, http://doi.wiley.com/10.1029/2009GL038973, 2009.

https://doi.org/10.5194/os-2020-112
Preprint. Discussion started: 16 December 2020

Lonergan, L. and White, N.: Three-dimensional seismic imaging of a dynamic Earth, Society, The Royal Transactions, Philosophical Sciences, Engineering, 357, 3359–3375, 1999.

Nakamura, Y., Noguchi, T., Tsuji, T., Itoh, S., Niino, H., and Matsuoka, T.: Simultaneous seismic reflection and physical oceanographic observations of oceanic fine structure in the Kuroshio extension front, Geophysical Research Letters, 33, 1–5, https://doi.org/10.1029/2006GL027437, 2006.

Nandi, P., Holbrook, W. S., Pearse, S., Páramo, P., and Schmitt, R. W.: Seismic reflection imaging of water mass boundaries in the Norwegian Sea, Geophysical Research Letters, 31, 1–4, https://doi.org/10.1029/2004GL021325, 2004.

Piété, H., Marié, L., Marsset, B., Thomas, Y., and Gutscher, M. A.: Seismic reflection imaging of shallow oceanographic structures, Journal of Geophysical Research: Oceans, 118, 2329–2344, https://doi.org/10.1002/jgrc.20156, 2013.

Ruddick, B. B., Song, H., Dong, C., and Pinheiro, L.: Water column seismic images as maps of temperature gradient, Oceanography, 22, 192–205, https://doi.org/10.5670/oceanog.2009.19, 2009.

Ruddick, B. R.: Seismic oceanography's failure to flourish: a possible solution, Journal of Geophysical Research: Oceans, 123, 4–7, https://doi.org/10.1002/2017JC013736, 2018.

Sallarès, V., Biescas, B., Buffett, G., Carbonell, R., Dañobeitia, J. J., and Pelegrí, J. L.: Relative contribution of temperature and salinity to ocean acoustic reflectivity, Geophysical Research Letters, 36, 1–6, https://doi.org/10.1029/2009GL040187, 2009.

Sheen, K. L., White, N., Caulfield, C. P., and Hobbs, R. W.: Estimating Geostrophic Shear from Seismic Images of Oceanic Structure, Journal of Atmospheric and Oceanic Technology, 28, 1149–1154, https://doi.org/10.1175/JTECH-D-10-05012.1, 2011.

Song, H. B., Pinheiro, L., Wang, D. X., Dong, C. Z., Song, Y., and Bai, Y.: Seismic images of ocean meso-scale eddies and internal waves, Chinese Journal Of Geophysics-Chinese Edition, 52, 2775–2780, https://doi.org/10.3969/j.issn.0001-5733.2009.11.012, 2009.

Talley, L. D., Pickard, G. L., Emery, W. J., and Swift, J. H.: Descriptive Physical Oceanography, Elsevier, 6th edn., 2012.

Tang, Q., Wang, C., Wang, D., and Pawlowicz, R.: Seismic, satellite, and site observations of internal solitary waves in the NE South China Sea, Scientific Reports, 4, 1–5, https://doi.org/10.1038/srep05374, 2014a.

Tang, Q. S., Gulick, S. P. S., and Sun, L. T.: Seismic observations from a Yakutat eddy in the northern Gulf of Alaska, Journal of Geophysical Research: Oceans, 119, 3535–3547, https://doi.org/10.1002/2014JC009938, 2014b.

Yilmaz, Ö.: Seismic data analysis: Processing, inversion, and interpretation of seismic data, Society of Exploration Geophysicists, 2001.